Research Article

Antonina N. Khanaychenko, Olga V. Nikolaeva, Olga A. Rylkova, Maria Saburova* and Vladimir V. Aleoshin

Genus *Proteomonas* is not monotypic: *P. agilis* sp. nov. (Cryptophyceae, Geminigeraceae) from the Black Sea and hidden diversity of *Proteomonas* species

https://doi.org/10.1515/bot-2024-0039
Received June 16, 2024; accepted September 6, 2024;
published online November 4, 2024

Abstract: The cryptophytes of the Black Sea are a poorly studied group that has yet to be fully resolved using comprehensive taxonomic approaches, including electron microscopy and molecular genetics. This study describes *Proteomonas agilis* sp. nov. belonging to a marine cryptophyte genus formerly thought to be monotypic. The morphological characters of the new species align with those currently used to delineate the genus *Proteomonas*, and are similar to those of the haplomorph *P. sulcata*, the type species, with minor morphological and molecular modifications. Phylogenetic relationships inferred from nuclear-encoded SSU, LSU, and ITS2 rDNA datasets confirmed that the new species belongs to the monophyletic genus *Proteomonas*, which is divided into two unequal branches. The largest and relatively long branch contains 18 strains, including *P. agilis* sp. nov. Comparison of ITS2 rRNA secondary structures using the compensatory base changes approach confirmed the distinction of *P. agilis* sp. nov. from the other *Proteomonas* strains. Our findings revealed that the cryptophyte genus *Proteomonas* is not monotypic but includes a range of unstudied species besides the type species *P. sulcata* and *P. agilis* sp. nov. described in this study. Therefore, an integrated approach is required for a careful revision of the genus.

Keywords: Cryptophyceae; *Proteomonas*; Black Sea; morphology; phylogeny

***Corresponding author: Maria Saburova**, Environment and Life Sciences Research Center, Kuwait Institute for Scientific Research, P.O. BOX 1638, Salmiya 22017, Kuwait, E-mail: msaburova@gmail.com
Antonina N. Khanaychenko and Olga A. Rylkova, A.O. Kovalevsky Institute of Biology of the Southern Seas, Russian Academy of Sciences, Leninskii Ave., 38/3, Moscow, 119991, Russian Federation, E-mail: a.khanaychenko@gmail.com (A.N. Khanaychenko), olga.rylkova@gmail.com (O.A. Rylkova)
Olga V. Nikolaeva, Belozersky Institute for Physico–Chemical Biology, Lomonosov Moscow State University, Leninskye Gory, 1/40, 119991 Moscow, Russian Federation, E-mail: olga_popova92@inbox.ru
Vladimir V. Aleoshin, Belozersky Institute for Physico–Chemical Biology, Lomonosov Moscow State University, Leninskye Gory, 1/40, 119991 Moscow, Russian Federation; Kharkevich Institute for Information Transmission Problems, Russian Academy of Sciences, Bolshoy Karetny Per., 19/1, 127051 Moscow, Russian Federation; and Faculty of Biology, Lomonosov Moscow State University, Leninskye Gory, 1/12, 119234 Moscow, Russian Federation, E-mail: aleshin@belozersky.msu.ru

1 Introduction

Cryptomonads, also known as cryptophytes or Cryptophyceae, are unicellular biflagellate protists, inhabiting fresh, brackish, and marine waters in coastal and oceanic ecosystems from the Arctic to the Antarctic. They play a crucial role in trophic links and the organic carbon cycle in aquatic ecosystems, particularly in coastal environments and meromictic basins (Cloern and Dufford 2005; Han and Furuya 2000; Hoef-Emden and Archibald 2017; Klaveness 1989; Medlin et al. 2017; Rammel et al. 2024; Shalchian-Tabrizi et al. 2008). Cryptophytes are traditionally thought to be low-light adapted as they are commonly found deep in the water column of lakes (e.g., Gervais 1998), under ice (Hammer et al. 2002), or in highly eutrophic waters (e.g., Adolf et al. 2006). They typically inhabit calm waters of meromictic basins and reach their maximum near the chemocline in the redox zone of the Arctic brackish water lakes (Krasnova et al. 2014) and of the Siberian lakes (Barkhatov et al. 2022). In the meromictic basin of the open Black Sea, two main peaks of cryptophyte biomass occur in the spring and summer. Spring peaks develop at a depth of 9–17 m with an irradiance ci. 10 % surface photosynthetically available radiance (SPAR), while during the summer, the cryptophycean maxima descend deeper to 30 m (1.5–2.5 % SPAR) at an absolute irradiance level of 2–5 mol photons m^{-2} d^{-1} (Mikaelyan et al. 2021).

Cryptophytes are among the most productive nanoflagellates found in aquatic environments, with their numbers varying from 10^2 to 10^7 cells l^{-1} among different water bodies, seasons and layers (Cerino and Zingone 2006; Han and Furuya 2000; Krasnova et al. 2014; Laza-Martínez 2012; Polikarpov et al. 2020; Šupraha et al. 2014; Xing et al. 2008). Cryptophytes contribute between 16.9 and 31.4 % of the total phytoplankton biomass in the China Seas coastal waters (He and Peng 2012). In Mediterranean coastal waters, they are relatively abundant, representing an average of 16.4 % and a maximum of 93.6 % of the total flagellate count at the beginning of September (Cerino and Zingone 2006).

Periodical blooms of cryptophytes (Johnson et al. 2016; Krasnova et al. 2014; Laza-Martínez 2012; Polikarpov et al. 2020; Šupraha et al. 2014) have never been considered toxic for living organisms. On the contrary, being a source of valuable essential chemical components such as lipids, polyunsaturated fatty acids, phycobiliproteins, and amino acids (Bermúdez et al. 2004; Dunstan et al. 2005; Oostlander et al. 2020; Peltomaa et al. 2018), cryptophytes are important prey for numerous heterotrophic organisms, including dinoflagellates, ciliates, rotifers, and copepods in various food webs (Aganesova 2021; Barkhatov et al. 2022; Coutinho et al. 2020; Johnson et al. 2016; Khanaychenko et al. 2018; Kim et al. 2020; Seixas et al. 2009; Zhang et al. 2013), especially in coastal environments. The highest grazing impact of microzooplankton on nanophytoplankton biomass, at 83 %, was observed for cryptophytes in late autumn in the coastal waters of Xiamen Bay in the China Sea (Huang et al. 2008). The abundant and very productive cyclopoid copepod *Oithona davisae* was found to have the highest selectivity of nanoplankton cryptophytes from the Black Sea coastal phytoplankton assemblages, with significant daily rations up to 140 % (Khanaychenko et al. 2018). Due to their valuable biochemical content, cryptophytes are commonly used as feed in aquaculture (Vu et al. 2016; Zhang et al. 2013). However, the taxonomic composition and trophic interactions of cryptophytes with other ecosystem components remain insufficiently investigated.

Cryptophytes are easily recognizable at the class level under the light microscope (LM) by their typical ovoid asymmetric cell shape, specific cell movement, gross morphology, and epifluorescence. However, their classification to the lower taxonomic levels can be challenging. A rapid assessment of cryptophyte abundance can also be achieved through a combination of pigment analysis by high-performance liquid chromatography (HPLC) and counting of the cells with high phycoerythrin fluorescence by flow cytometry (FCM), though only at the class level (Moorhouse et al. 2018).

To distinguish between species, early taxonomists have traditionally used unique morphological features of cryptophyte cells visible under high resolution LM, including the cell shape and size, the shape and position of the chloroplast, the number and position of pyrenoid(s), the shape of the furrow/gullet, and the number of ejectosomes (Clay et al. 1999). However, only electron microscopy (EM) can reveal certain characters of significant taxonomic value such as the furrow/gullet complex, ultrastructural features of flagella, position of nucleomorph, morphology of pyrenoid, type and structure of periplast, etc (Deane et al. 2002). Some early studies also suggested the use of cryptophyte cell color as a taxonomic identification key, in addition to morphological characters (Clay et al. 1999). However, the color of cryptophyte cells varies significantly depending on the cell life stage and culture conditions, may be influenced by light quality and nitrogen sources, resulting in changes in the proportions of chlorophyll and phycoerythrin content in their plastids (Latsos et al. 2021).

Although LM and EM-based descriptions have been successfully used in taxonomy and systematic studies of cryptophytes to characterize them precisely, the discovery of haploid and diploid morphs of the same species with contrasting morphological features, such as in *Proteomonas sulcata* D.R.A. Hill *et* Wetherbee (1986) and *Teleaulax amphioxeia* (W. Conrad) D.R.A. Hill/*Plagioselmis prolonga* Butcher ex Novarino, Lucas *et* Morrall 1994 (Altenburger et al. 2020), along with further detection of numerous *Cryptomonas*/*Campylomonas* dimorphic strains (Hoef-Emden and Melkonian 2003) have significantly disrupted the previous systematic scheme.

The class Cryptophyceae was thought to consist of 20 genera and 100 species, identified on the basis of rRNA tree (Hoef-Emden and Melkonian 2003; Hoef-Emden et al. 2002; Marin et al. 1998). However, recent studies suggest that the true species diversity of the group is underestimated and apparently far exceeds these estimates, and precise species identification and taxonomy remain unresolved (Hoef-Emden and Archibald 2017). Recently, new genera and species of freshwater (Gusev et al. 2020; Hoef-Emden 2018; Laza-Martínez 2012) and marine (Daugbjerg et al. 2018; Khanaychenko et al. 2022; Laza-Martínez et al. 2012; Magalhães et al. 2021; Majaneva et al. 2014) cryptophytes have been described in addition to previously known taxa, and some old species have been emended. New cryptophyte species was recently isolated from an unusual environment, tropical forest soil in a biosphere reserve in Vietnam (Martynenko et al. 2022).

Documenting marine cryptophyte biodiversity remains a global challenge. For instance, cryptophytes (identified at the class level) were found to be the primary contributors of phytoplankton biomass during the autumn and winter months in the China Seas (Sun et al. 2022). However, taxonomic studies of this group in this area are limited, with only six marine species documented, misidentified as belonging to the freshwater genus *Cryptomonas* Ehrenberg

(Hu et al. 2002). Studies on the diversity of cryptophytes in the Black Sea also are few and mainly restricted to identification based on the morphology of the fixed cells distinguishable under a light microscope. Researchers report varying numbers of cryptophytes in different areas of the Black Sea, ranging from a few to 20 species, with most of them erroneously assigned to the genus *Cryptomonas* (Mikaelyan et al. 2020; Moncheva et al. 2019; Rouchijajnen 1967, 1970). However, modern integrative studies have shown clearly that the genus *Cryptomonas* is exclusively composed of freshwater species (Gusev et al. 2020; Hoef-Emden and Melkonian 2003).

Consequently, imprecise and invalid specific and generic names of the cryptophytes are commonly used worldwide, including studies in the Black Sea. To achieve precise identification of cryptophytes, integrative studies that include mandatory molecular genetic data are necessary (e.g., Łukaszek and Hoef-Emden 2017; Solarska et al. 2023). Such an integrative study was conducted to identify the species in a recently established collection of cryptophyte clonal cultures isolated from the Black Sea. This study resulted in the description of a new Black Sea cryptophyte species, *Rhodomonas storeatuloformis* (Khanaychenko et al. 2022).

The marine cryptophyte genus *Proteomonas* D.R.A. Hill et Wetherbee (1986) is noteworthy for described alternating haploid and diploid morphs in its type species, *Proteomonas sulcata* (Hill and Wetherbee 1986). The genus was once thought to be monotypic, forming an independent lineage with weak affinity to any other cryptophyte clade (Marin et al. 1998). It has since been proposed to be attributed to its own subfamily, the Proteomonadoidae (Greenwold et al. 2023). To date, no other species related to *P. sulcata* have been described, and this cryptophyte has never been previously reported among the phytoplankton composition of the Black Sea. Our aim was to carry out integrative studies to identify a new strain isolated from the Black Sea coastal waters and to find out its potential relationship with *P. sulcata* based on light and scanning electron microscopic observations and phylogenetic analyses of the ITS region and the 18S and 28S nuclear rDNA genes sequences.

2 Materials and methods

2.1 Origin and isolation

The strain IBSS-Cr-4.14M was isolated from a sample collected from the coastal area of the NW Black Sea (44.37 N 33.3118 E) at a depth of 0–1 m in October 2019 by A.N. Khanaychenko and D.V. Moiseenko, Institute of Biology of Southern Seas (IBSS). The cryptophyte culture was established using the dilution method and subsequently subcultured several times through single cell isolation by micropipetting. It was then maintained in the IBSS collection of live cryptophyte cultures until the morphological and molecular analyses were conducted.

2.2 Culture maintenance

Since isolation, the strain has been purified and deposited in monospecific culture at the Culture Collection of Marine Cryptophytes (CCMC) at IBSS. The non-axenic culture of the strain was routinely maintained at an irradiance of 5–10 µmol photons m^{-2} s^{-1} under a 12:12 light:dark photoperiod at a temperature of 22 ± 2 °C. The culture was diluted weekly with half Walne's medium prepared from filtered (0.22 µm) and sterilized Black Sea seawater (salinity 18) to support exponential growth (Andersen 2005).

2.3 Light microscopy (LM)

Live cells were isolated by micropipetting and transferred to a glass slide in a live drop for observation under high magnification LM. Live cells were observed under inverted Nikon Eclipse MS 100 and Nikon Eclipse TS2R (Nikon Metrology NV) light microscopes equipped with Nomarski differential interference contrast (DIC) optics. LM images were taken with an Infinity 3 Luminera color digital camera at 400 × magnification and under oil immersion in a live drop at 1,000× magnification. Cell dimensions, the presence of various inclusions, the position of the pyrenoid and the shape of the plastid were examined from more than 200 live cells.

2.4 Scanning electron microscopy (SEM)

A volume of 2 ml of dense (ci. 10^5 cells ml^{-1}) culture of the strain IBSS–4.14M was fixed in acidified 1 % Lugol's solution for 60 min (Bistricki and Munawar 1978; Dolgin and Adolf 2019). After fixation, the sample was gently concentrated under a low vacuum (<0.2 atm) onto a polycarbonate filter (2-µm pore size, Dubna, Russia) using a filter funnel (Sartorius, Germany). After precipitation on a filter, the cells were rinsed three times with distilled water and then dehydrated gradually in a graded ethanol series. The filters were dried using automated critical point dryer Leica EM CPD300 (Leica Microsystems, Germany) for 1.5–2.5 h. The dried filters were mounted on aluminum stubs using carbon adhesive tabs and sputter-coated with Au/Pd using vacuum

coater Leica EM ACE200 for 1.0 min before examination in a scanning electron microscope Hitachi SU3500 (Hitachi High Tech, Japan). Cell length, width, and depth were measured on SEM micrographs of randomly selected cells using ImageJ ver. 1.50i (National Institute of Health, USA), and the range, mean values and standard deviation were calculated.

2.5 Pigment absorption measurement

The phycoerythrin absorption maximum was assessed using the "quantitative techniques on wet filters" method (Mitchell and Kiefer 1988) in accordance with Efimova et al. (2020). For the whole-cell absorption measurements, an aliquot of the culture was gently filtered under low vacuum (<0.2 atm) onto the glass fiber filters (Whatman GF/F). The optical measurements were performed using a dual-beam spectrophotometer Lambda 35 (Perkin Elmer) equipped with an integrating sphere at wavelengths between 350 and 750 nm.

2.6 DNA extraction, PCR, and sequencing

Total genomic DNA was extracted from the strain IBSS-Cr-4.14M using the DIAtom DNA Prep Kit (Isogen, Russia) following the protocol provided by the manufacturer. Partial nuclear encoded 18S (SSU) and 28S (LSU) rDNA and complete internal transcribed spacer (ITS) regions were amplified with novel and described earlier primers (Table 1) with Encyclo PCR kit (Evrogen, Russia). PCR cycling conditions included denaturation at 95 °C for 5 min, followed by 40 cycles of denaturation at 95 °C for 30 s, annealing at 55 °C for 30 s, extension at 72 °C for 3 min, and final extension at 72 °C for 5 min. PCR products were separated by 0.8 % agarose gel electrophoresis and purified using Cleanup Mini Kit (Evrogen, Russia). Amplicons were directly sequenced with an Applied Biosystems 3730 DNA Analyzer. The sequence of the strain IBSS-Cr-4.14M was deposited in the GenBank with accession number OR687719.

2.7 Phylogenetic analyses

Partial nuclear SSU and LSU rDNA genes, complete 5.8S gene, and complete ITS1 and ITS2 spacers were obtained from the strain IBSS-Cr-4.14M as a set of overlapping sequences to clarify the phylogenetic relationship of this strain as a novel cryptophyte species *P. agilis*. The assembled contig was 3,912 bp in length. Each *P. agilis* gene was separately aligned with corresponding genes from eighteen *Proteomonas* strains, five uncultured clone sequences affined to *Proteomonas* according to BLAST search, and *Geminigera cryophila* and *Teleaulax amphioxeia* as an outgroup species. For tree inferences, three alignments (SSU, 5.8S, and LSU) were concatenated. Bayesian phylogenetic inference (BI) was performed using MrBayes 3.2.6 with four runs under the GTR + I + G4 model of evolution, 5,000,000 generations and 50 % burn-in. Maximum likelihood (ML) inference was performed using IQ-TREE (Nguyen et al. 2015) under the ModelFinder search (–m MFP) and ultrafast bootstrap (–bb 1000). GenBank accession numbers for the gene sequences of strains employed in the Bayesian and ML phylogenetic analyses are listed in the Supplementary Table S1.

ITS2 sequences for four *Proteomonas* strains were assembled from GenBank SRA libraries SRR1300355, DRX303455, DRX303452, and ENA SAMN35743121 with SPAdes (Bankevich et al. 2012) after trimming the adapter sequences from the read data with Trimmomatic (Bolger et al. 2014) (Supplementary Table S2). The secondary structures of nucleus–encoded ITS2 sequences of the strain IBSS-Cr-4.14M (*P. agilis* sp. nov.) and three *Proteomonas* strains were predicted using the RNA folding program available at the mfold server (http://mfold.rna.albany.edu/?q=mfold/RNAFolding–Form) (Zuker 2003) with default values. All predicted structures of ITS2 were manually examined and compared for common stems, loops, and bulges. Compensatory base changes (CBCs) in different helices were manually identified from the ITS2 secondary structures.

Table 1: Primers used for PCR and sequencing.

Gene	Primer	Sequence	Reference
18s	A	5′-GTATCTGGTTGATCCTGCCAGT-3′	Medlin et al. (1988)
18s	18r3	5′-CAACTACGAGCTTTTTAAC-3′	This study
18s	18r5	5′-TGGTGCCCTTCCGTCAAT-3′	This study
18s	d6	5′-CCGTTCTTAGTTGGTGG-3′	Simdyanov et al. (2015)
18s	d71	5′-GTCCCTGCCCTTTGTACACACCGCCCG-3′	Simdyanov et al. (2017)
28s	NLR 204/21	5′-ATATGCTTAARTTCAGCGGGT-3′	Van der Auwera et al. (1994)
28s	D2dnB	5′-CCTTGGTCCGTGTTTCAAGAC-3′	Kjer et al. (2001)
28s	R1411sq	5′-GTTGTTACACACTCCTTAGCGG-3′	Medina et al. (2001)

3 Results

3.1 Taxonomy

Proteomonas agilis Khanaychenko, Nikolaeva, Rylkova, Aleoshin, Saburova *et* Moiseenko sp. nov. (Figures 1–3).

3.1.1 Description

Cells are oval, slightly convex and dorsoventrally flattened, obloid in shape; with rounded apical and antapical ends, semicircular in transverse section, with slightly convex dorsal and slightly concave ventral surfaces. Under LM,

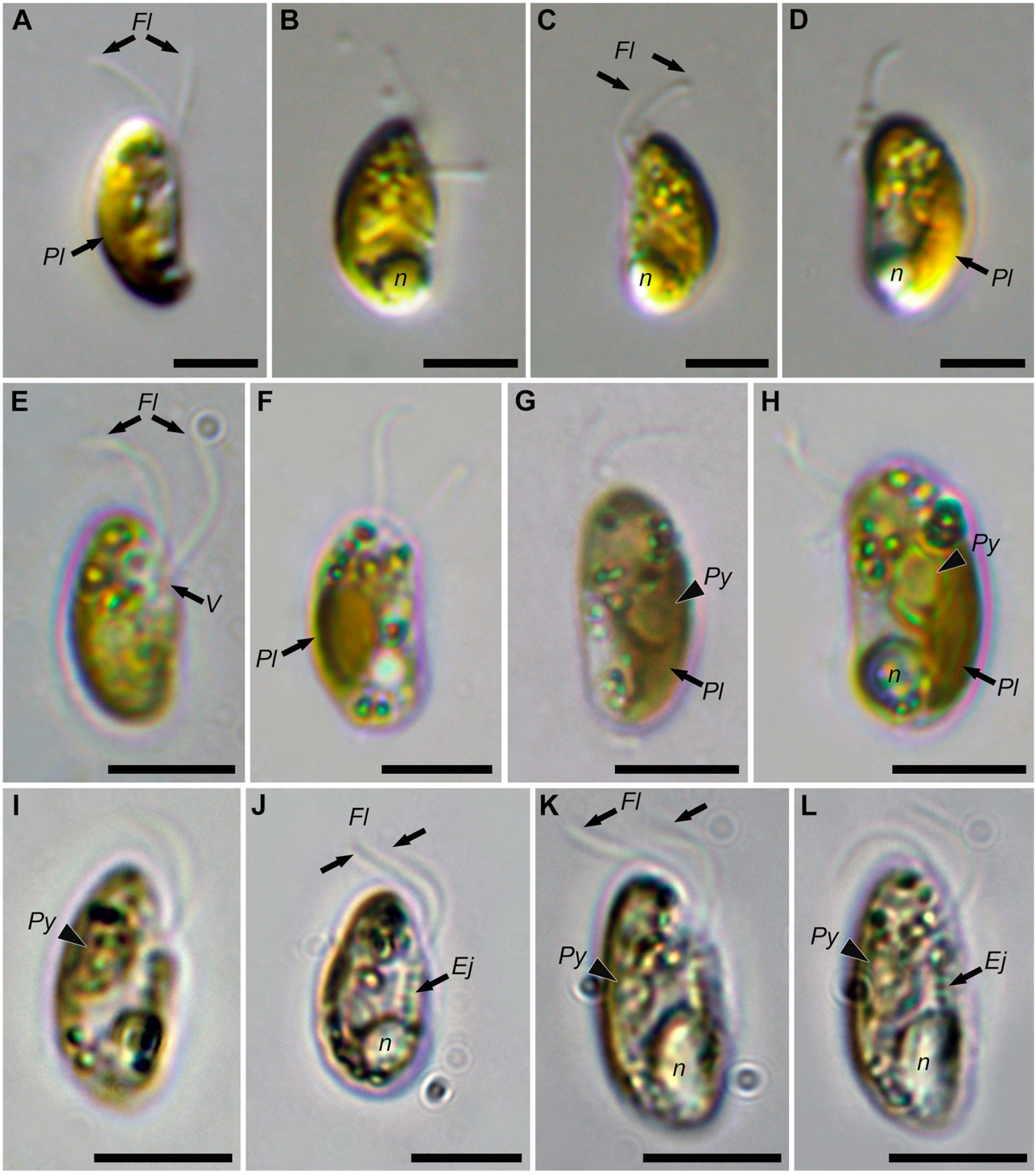

Figure 1: Light micrographs of *Proteomonas agilis* sp. nov. (strain IBSS-Cr-4.14M). (A, B, E, F, and I–L) Lateral right-sided view. (C, D, G, and H) Lateral left-sided view. Cells at different focal planes showing two flagella (Fl), single plastid (Pl), large single pyrenoid (Py), posterior nucleus (n), vestibulum (V), and row of large ejectosomes lining gullet (Ej). Scale bars = 5 μm.

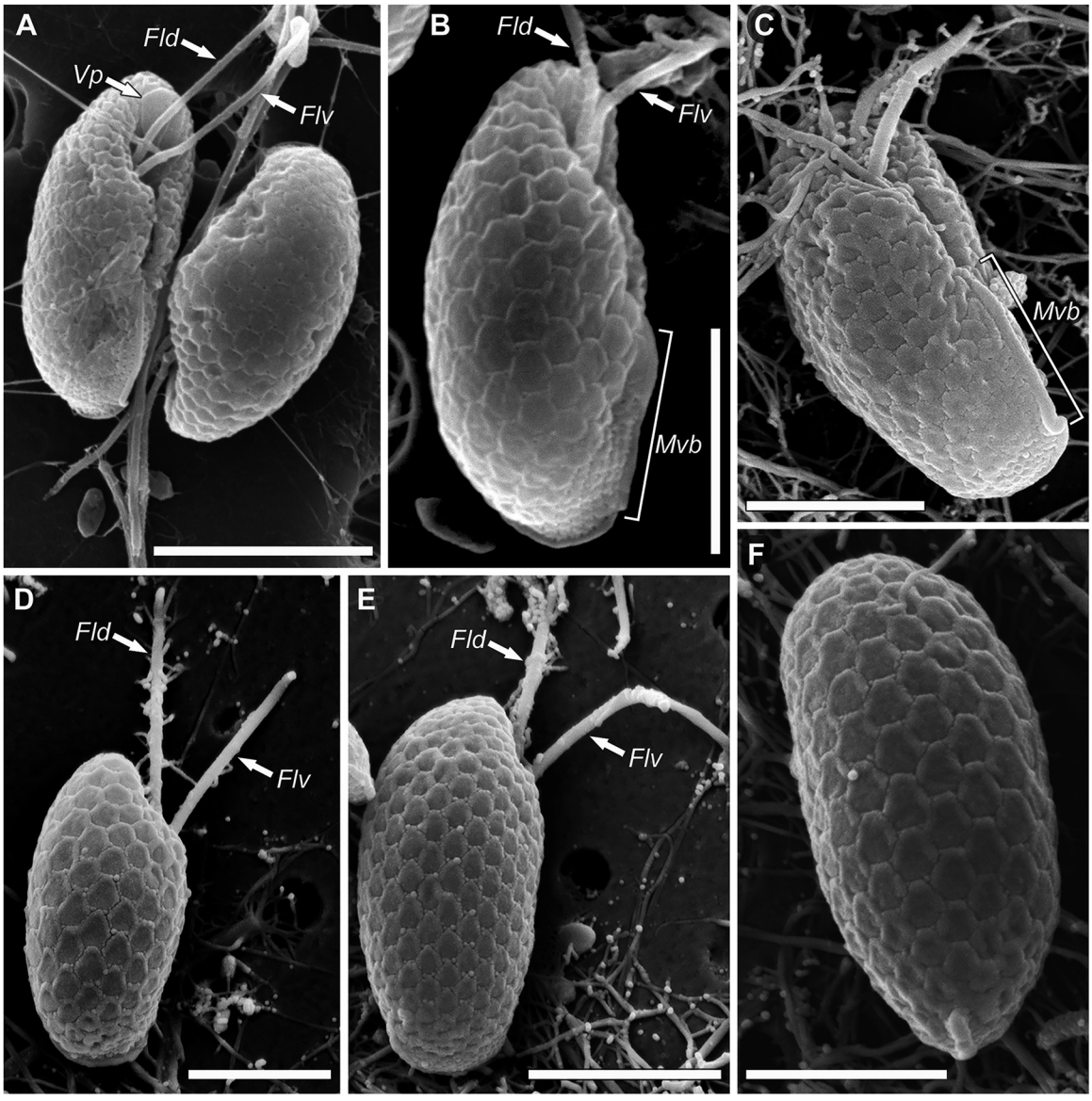

Figure 2: SEM micrographs of *Proteomonas agilis* sp. nov. (strain IBSS-Cr-4.14M). (A–C) Ventro–lateral right-sided view showing dorsal (Fld) and ventral (Flv) flagellum, vestibular plate (Vp), ventral furrow, and mid-ventral band (Mvb). (D and E) Lateral right-sided view showing two unequal flagella. (F) Dorsal view showing the inner periplast component consists of an ordered system of discrete, anteriorly stepped hexagonal plates. Scale bars = 5 µm (A, D, and E) and 3 µm (B, C, and F).

living cells range from 7 to 10 µm in length and from 3 to 4 µm in width, width to length proportions ci. 0.5; with a single oblique plastid/chloroplast with PE-545, and a free pyrenoid positioned ventrally beside it. SEM revealed two unequal flagella, the dorsal longer than the ventral one, are shorter than the cell length, curved up and backwards, positioned on an upper 1/3 ventral side from a subapical vestibulum elongated by the oblique furrow extending 1/2 cell length; IPC is covered by discrete, hexagonal 'plates', fixed posteriorly, raised to accommodate small underlying ejectosomes, while discharged forming distinct pores. Mid-ventral band 1/2 cell length from antapex to furrow opening is evident in young cells just after cell division by pole reversal. Cysts and palmeloid forms were not observed.

3.1.2 Holotype

The SEM stub containing fixed, critical point dried material from the strain IBSS–Cr-4.14M (*P. agilis* sp. nov.) was deposited at the Algal Herbarium (LE) of the Komarov

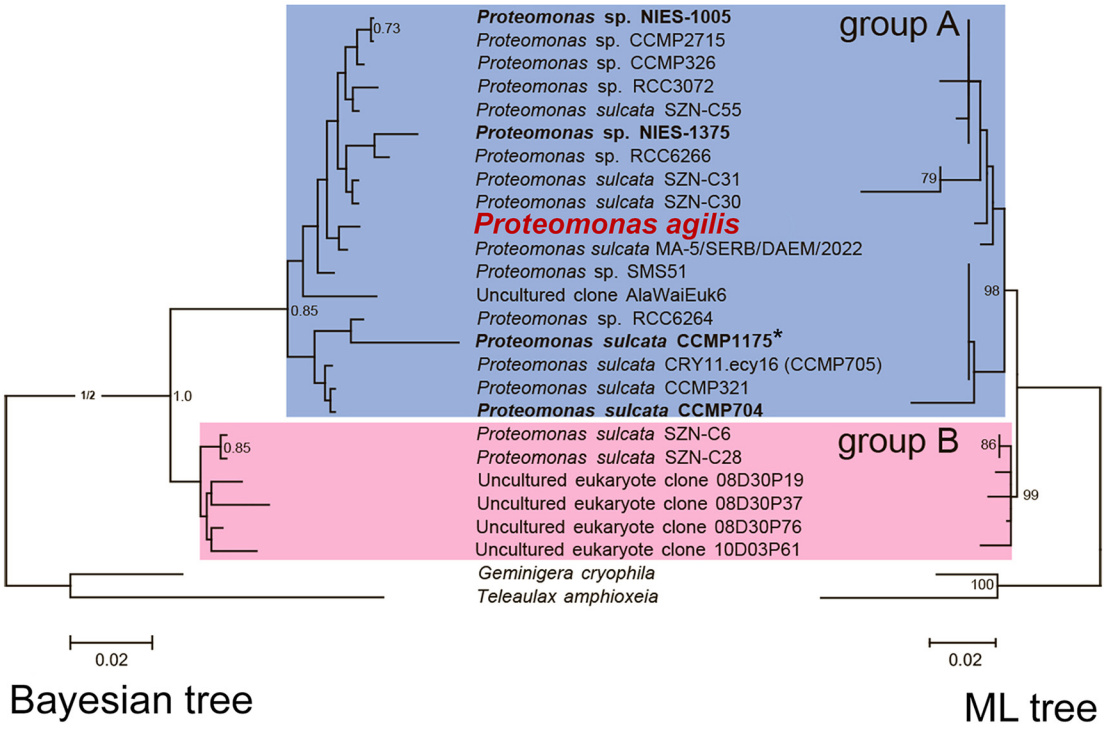

Figure 3: Bayesian and maximum likelihood (ML) trees based on the concatenated nuclear-encoded SSU, 5.8S, and LSU rRNA genes of *Proteomonas* species. Bayesian posterior probabilities are shown near the internal nodes. Posterior probabilities and bootstrap values which are lower than 0.7/70 are not shown. *Proteomonas agilis* sp. nov. (strain IBSS-Cr-4.14M) is highlighted in red font; the asterisk marks the type strain of *P. sulcata*; taxa in bold type are strains involved in the compensatory base changes analysis in ITS2 rDNA secondary structures (see Figure 5). Scale bar: substitutions per site.

Botanical Institute, St. Petersburg, Russia (identification number LEA0004142).

3.1.3 Type locality

Coastal waters of the NW Black Sea (44°37′00″N; 33°31′18″E); the strain IBSS–Cr-4.14M was isolated in late October 2019 by A.N. Khanaychenko and D.V. Moiseenko.

3.1.4 Authentic strain

The strain IBSS–Cr-4.14M is deposited at the Culture Collection of Marine Algae (CCMA) of IBSS and maintained on a regular basis at the Culture Collection of the Black Sea Cryptophytes (CCBSC) in the Department of Aquaculture and Marine Pharmacology of IBSS. The glutaraldehyde and alcohol fixed samples of the strain IBSS–Cr-4.14M are also kept in the Department of Aquaculture and Marine Pharmacology of IBSS.

3.1.5 Gene sequence

DNA sequence is deposited in GenBank under accession number OR687719 (nuclear SSU, ITS, and LSU rDNA).

3.1.6 Habitat

Marine coastal waters, plankton.

3.1.7 Etymology

Epithet from the Latin adjective "*agilis*" because of the sudden, fast, nimble movements in different directions typical of this species.

3.2 Morphological observations

3.2.1 Culture

The color of the cultures of *P. agilis* sp. nov. (strain IBSS-Cr-4.14M) with cell concentration higher than 10^5 cells ml^{-1} was pink-brown in exponentially growing cultures at irradiance <10 µmol photons m^{-2} s^{-1} and temperature 18–24 °C, and gradually changed to light brownish and up to yellow-greenish when exposed to the irradiance >15 µmol photons·m^{-2}·s^{-1} and increased temperature (>25 °C). The color of the culture depended on the variation of the light spectrum, cell density, and culture age, which affected the ratio of

chlorophyll to phycoerythrin in the cell. The absorption spectrum of the IBSS-Cr-4.14M strain cells, as determined by spectrophotometry, exhibited an absorption maximum at 538–551 nm, which is characteristic of the cryptophyte phycoerythrin Cr-PE 545 absorption range (Greenwold et al. 2019). The high content of phycoerythrin was confirmed by the distinct orange fluorescence of the cells with a strong emission peak at 545 nm due to the presence of Cr-PE 545, as detected by spectrophotometry. The overall results of phycoerythrin-specific light absorption characteristics in a range of new cryptophyte species will be presented in a separate article.

3.2.2 Cell behavior (LM)

Living cells in a droplet under quiescent conditions are often observed to be attached to the glass surface (probably by flagella) in an upright position with the apical side down and fluttering, trembling in the attached position. Slightest vibration resulted in abrupt cell sideways jumps of the cells, apparently due to the sharp "shooting" of their ejectosomes, followed by rapid swimming with abrupt changes of direction.

3.2.3 General morphological features

P. agilis sp. nov. occurs in culture only as live motile cells. Measured under LM at 400× magnification, live cells vary in length from 7 to 10.5 µm and in width from 2.5 to 4 µm, width to length ratio ci. 0.5. Measured from the SEM micrographs, the cells vary from 5.2 µm in length, 2.3 µm in width, and 2.9 µm in depth in the young specimens after cytokinesis to 10.2 µm (length), 5.2 µm (width), and 4.9 µm (depth) in the mature cells. Mean SEM cell sizes (n = 40) in the exponential growth phase are 7.1 ± 0.9 µm (length), 3.4 ± 0.5 µm (width), and 3.5 ± 0.3 µm (depth).

In dorsal and ventral view, the cells are obovate with a rounded anterior end and a rounded but slightly tapered posterior end. Due to a slight lateral flattening, most of the cells were observed lying on one side. They are slightly convex in lateral view, with minor dorso-ventral compression, a slightly convex dorsal surface and slightly concave ventral surface. The anterior and posterior ends of the cell are rounded (Figures 1 and 2). Two unequal flagella, the dorsal longer than the ventral, directed upward and dorsally, are inserted laterally into a cavity from a shelf-like area on the ventral right side of the vestibulum (Figures 1A, 1C, 1E, 1J, 1K and 2A, 2B, 2D, 2E). The classic cryptomonad asymmetric vestibulum is present (Figure 1E–A). Along the ventral surface of the cell, posteriorly from the inner depression of vestibulum, from almost one third of the cell length from the apex, a prominent furrow extends longitudinally along the ventral surface for about 1/3 to 1/4 of the cell length (Figure 2A–C). Rows of extruded ejectosomes follow the furrow, and are also found in other areas of the cell (Figure 1J–L).

A single parietal oblique plastid, filling almost the entire cell on the dorsal side and tapering ventrally, is not connected to a single free pyrenoid located close to the center of the cell (Figure 1A, D, F–I, K, and L). A large globular nucleus located in the antapex, is visible at any position of the cell (Figure 1B–D, H, and J–L). A vestibular plate, resembling a flat tongue, is visible only in young cells, just after cell division, when viewed from the ventral side, and is located on the posterior wall of the vestibulum, just behind the dorsal, longer flagellum (Figure 2A). Mid-ventral band, extending for 1/2 of the cell length from the antapex to the furrow opening, is clearly visible in young cells just after cell division (Figure 2B and C).

The inner periplast component consists of an ordered system of discrete, anteriorly stepped hexagonal plates, resembling fish scales in some cells. Rows of hexagonal plates cover the entire cell including the antapex (Figure 2B–F). Young (small) daughter cells just after cytokinesis show slightly undeveloped hexagonal plates, especially, in the area of the so-called anamorphic zones around the edges of the divided cells near the vestibulum and along the mid-ventral band, which is only visible just after division in the posterior part of young cells when viewed laterally. Pores after discharged ejectosomes are visible at the corners of some plates, especially in young cells (Figure 2A).

Direct LM observation of living cultured cells revealed a reorientation of the daughter cell relative to the parent cell during cell division, termed pole reversal. This occurred during the cytokinesis, whereby the posterior of the developing daughter cell was formed from the anterior of the parent cell. Separated by rotation relative to each other, the daughter cells were significantly smaller than the mature cells.

3.3 Molecular phylogeny

According to both Bayesian and ML phylogenetic trees of *Proteomonas* species (Figure 3), the genus *Proteomonas* is monophyletic and divided into two unequal groups: group A with a relatively long branch (18 strains including *P. agilis*) and group B (six strains). The various strains assigned to *P. sulcata* do not form a single group on either the BI or ML

trees. Fortunately, the type strain of *P. sulcata* (CCMP1175) has been characterized by marker genes, so we can distinguish true *P. sulcata* from misattributed strains. Only few nodes have high posterior probability and bootstrap value greater than 0.7/70, probably due to high similarity between sequences. Among group A strains, the tree is represented by SSU from 17 strains, 5.8s from 8 strains, and LSU from 9 strains, with SSU similarity level greater than 98 %. Group B strains represent only SSU with a similarity level more than 99.5 %. Although new species *P. agilis* (strain IBSS-Cr-4.14M) is closely related to several *Proteomonas* strains, it differs from them in the rRNA genes and ITS sequences.

3.4 Secondary structures of nuclear ITS2 regions

ITS2 of the strain IBSS-Cr-4.14M folded into four predicted helices as in most eukaryotes (Coleman 2007), with the longest helix III, and a typical mismatch U–U in helix II (Figure 4). To confirm that the strain IBSS-Cr-4.14M is a distinct species, we compared its nuclear ITS2 structure (Figure 4) with homologous ITS2 structures of *Proteomonas* strains for detection of CBCs.

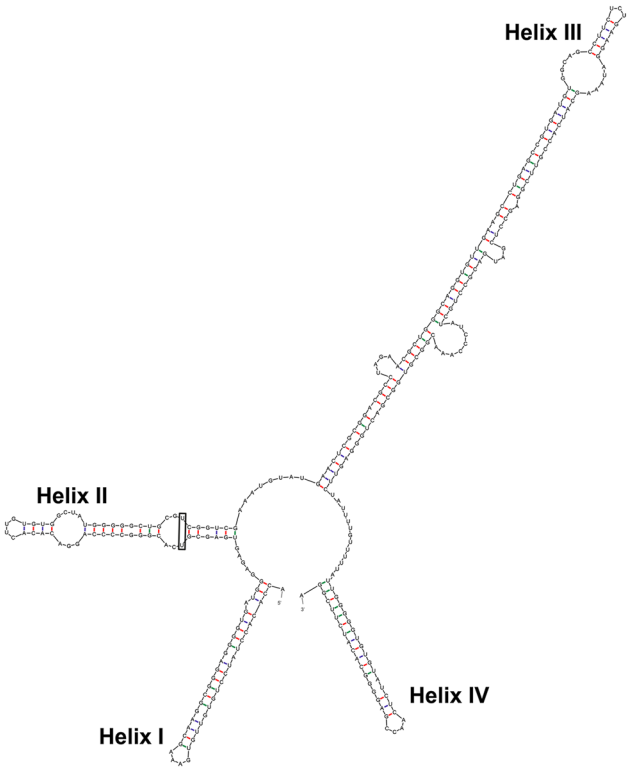

Figure 4: Predicted secondary structure of ITS2 for *Proteomonas agilis* sp. nov. (strain IBSS-Cr-4.14M). Helices are numbered according to Coleman (2000). Typical unpaired U–U in helix II is marked by a rectangle.

At the time of analysis, no ITS2 sequences from any *Proteomonas* strain were available in GenBank. However, Sequence Read Archive (SRA) libraries for the three strains (*P. sulcata* CCMP704, *Proteomonas* sp. NEIS-1375, and *Proteomonas* sp. NEIS-1005) allowed us to assemble their ITS2 sequences (Supplementary Figures S1–S3). One of the SRA libraries belongs to a single nominal *Proteomonas* species with molecular data, *P. sulcata* CCMP704 (Marin et al. 1998). Additional *P. sulcata* strain data, specifically *P. sulcata* CCMP1175 (type strain collected in the Bass Strait off the coast of Cape Otway, Victoria, Australia in the 1980s by D.R.A. Hill (Hill and Wetherbee 1986), sample accession: SAMN35743121), was obtained from the European Nucleotid Archive (ENA) database (https://www.ebi.ac.uk/ena/). Data on ITS2 of *Proteomonas* strains NIES-1005 and NIES-1375 were found in the Gene database, originated from the Microbial Culture Collection at the National Institute for Environmental Studies (NIES) of Japan, established in 1983.

CBCs between IBSS-Cr-4.14M and four other *Proteomonas* strains were found in all four ITS2 helices, but for the easier perception, we only provide visualization for helix II (Figure 5). The ITS2 structures of two *P. sulcata* strains, CCMP704 and CCMP1175, were found to be identical, proving the identity of both with the original type species of the genus, *P. sulcata*, isolated from the south-eastern Australian coastal waters (Hill and Wetherbee 1986).

In general, in all *Proteomonas* strains, helix II splits into two parts – conservative proximal and variable distal (Figure 5). The conservative part contains the identical motif and the typical mismatch U–U. The variable part differs among the strains in length, number of complementary pairs, and number and type of unpaired bases. Terminal loops are conserved in length among strains. Helix II in *Proteomonas* NIES-1375 is the longest among four strains, and has a bulge. Helix II in IBSS-Cr-4.14M is slightly shorter and has an internal loop, while Helix II in *Proteomonas* NIES-1005 and *P. sulcata* CCMP704/CCMP1175 have no internal loops, or bulges. In addition, helix II in *P. sulcata* CCMP704 and CCMP1175 is shortened in both the conservative and variable parts, making the homologation of base pairs between *P. sulcata* CCMP704/CCMP1175 and other strains difficult. CBCs are present only in the variable part; all strains have numerous CBCs (Table 2) and, should therefore be considered as separate species.

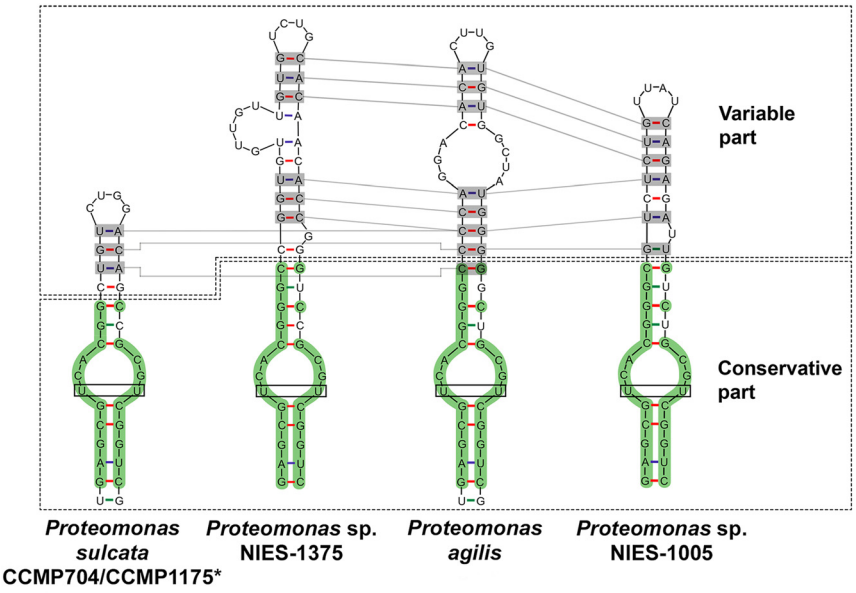

Figure 5: Predicted secondary structure of ITS2 helix II for *Proteomonas sulcata* (strains CCMP704 and CCMP1175), *Proteomonas agilis* sp. nov. (strain IBSS-Cr-4.14M), and *Proteomonas* spp. (strains NIES-1375 and NIES-1005). Typical unpaired U–U is marked by a rectangle. Conservative motifs are marked in green; compensatory base changes (CBCs) are marked by rectangular boxes highlighted with gray background; the asterisk marks the type strain of *P. sulcata*.

Table 2: Number of compensatory base changes (CBCs) in ITS2 between *Proteomonas agilis* (strain IBSS-Cr-4.14M) and three closely related *Proteomonas* strains.

Strain	Helix I	Helix II	Helix III	Helix IV	Total
Proteomonas sulcata CCMP704/CCMP1175	7	3	11	6	27
Proteomonas sp. NIES-1375	5	6	1	9	21
Proteomonas sp. NIES-1005	11	6	2	2	21

4 Discussion

The initial description of the genus *Proteomonas* was based on a single species isolated from the south-eastern Australian coastal waters, with the holotype designated *P. sulcata* (Hill and Wetherbee 1986). The authentic strain had an unusual life history with alternating morphology between the haplomorphic and diplomorphic forms, identified as haploid and diploid life stages. However, that study found that the haplomorph and diplomorph, which differed in size, periplast structure, configuration of the flagellar apparatus, and the quantity of nuclear DNA, both reproduced by simple cell division, and each was capable of producing the other cell type (Hill and Wetherbee 1986). The only other species, *Proteomonas pseudobaltica* (Erata *et* Chihara) Novarino 1991, which the author believed to be a diplomorphic life stage of a species belonging to the genus *Proteomonas*, was described only morphologically (Novarino 1991), based on the specimens isolated by Butcher in 1961 from a marine rock pool on the Channel Islands. Initially, this cryptophyte was identified as *Cryptomonas pseudobaltica* Butcher 1967 (a strain 979/9 from the Culture Collection of Algae and Protozoa, U.K., CCAP). Thus, to date, the morphology of only two species of the genus *Proteomonas* has been described: the dimorphic *P. sulcata* (Hill and Wetherbee 1986) and *P. pseudobaltica* (Novarino 1991), the latter pretending to belong to the genus *Proteomonas.*

In the present study, we have attempted to compare selected morphological characters used to delineate taxa for different strains of *Proteomonas*, summarized in Table 3. Besides the morphological description of dimorphic *P. sulcata* strains (Cerino and Zingone 2006; Hill and Wetherbee 1986) and *P. pseudobaltica* (Novarino 1991), we included the morphological characters of the described new species, *P. agilis* sp. nov., and the cryptophyte species with very similar morphological description based only on LM observations, found in the same vicinities as *P. agilis,* but in the early 1970s, named *Cryptomonas flexa* (Rouchijajnen 1970). All described strains, except the last one for which no data were available, have the accessory pigment CrPE545 in the phycobiliprotein.

The morphological characteristics of *P. pseudobaltica*, described by Novarino (1991) differ significantly from those

Table 3: Comparison of selected (LM and SEM-observed) morphological characters used to delineate the taxa within the family Geminigeraceae between *Proteomonas agilis* sp. nov., related (generi)type-species and cryptomonads from the Black Sea described by Rouchijajnen (1970).

Character	*Proteomonas* agilis sp. nov.[d]	*Proteomonas sulcata* (haplomorph)[e]	*Proteomonas sulcata* (diplomorph)[e]	*Proteomonas sulcata* (haplomorph)[f]	*Proteomonas pseudo-baltica* (diplomorph)[g,h]	*Cryptomonas flexa*[b,i]
Cell shape[a]	Oval/obloid in transverse section	Tear-shaped, slightly compressed	Ovate to elliptic	Falcate	Ovoid	Obconical, dorsoventrally compressed
Apical end	Rounded	Rounded	Distinctly pointed	Rounded	Obliquely truncate or slightly rostrate	Slightly pointed
Antapical end	Rounded	Rounded	Subacute to rounded	Acute tail	Sub-obtuse	Subacute
Dorsal surface	Convex	Convex	Convex	Convex	Convex	Convex
Ventral surface/margin	Slightly concave	Flat/straight	Convex	Concave	Convex	Slightly concave
Cell size, µm (alive, LM)	7–10 × 3–4	7.5–10.5 × 4–6	10–14 × 5–7	5.5–8.8 × 2–5	21.7 × 10[g] 18–30 × 5–8[h]	8–12 × 5–6
Cell size, µm (SEM)	7.1 ± 0.9 (length) 3.4 ± 0.5 (width) 3.5 ± 0.3 (depth)	NA	NA	NA	8.8–16.9 × 4.9–9.6[g]	NA
Plastid number[a], shape, position	Single parietal, crossing entire cell	Single, parietal, occupying entire length from dorsal margin and 1/2 length of ventral margin	Single, parietal, extending the length of the cell dorsally and about half the length ventrally	Single, parietal	1 or 2, parietal, much lobed, occupying most of the cell	Single dorsal, lining diagonally from left to right, edges bent ventrally
Pyrenoid	Single, centrally located	Single, with an entire starch coating, located mid-dorsally	Central, dorsal, with an entire starch sheath	NA	Single with obvious starch sheath	NA
Flagella length	Unequal, 4/5 (dorsal) and 2/3 (ventral) cell length	Unequal	Unequal	Subequal	Equal, slightly less than cell length	Equal, 1/2 cell length
Flagella position	Upper 1/3 ventral side, curved up- and backwards	Upper ventral side, from a shelf-like region on the right side of vestibulum, anteriorly directed	Upper ventral side, from a shelf-like region on the right side of vestibulum, anteriorly directed	Middle ventral side, curved ventrally-anteriorly	Upper ventral side	Inserted laterally, up- and backwards
Furrow[a]	Oblique, 1/2 cell length	c.a. 1/4 cell length	Slightly oblique, c.a. 1/3 cell length	1/2 to 3/4 cell length	Short	2/3 cell length
Vestibular plate[a]	Flat, tongue-like, on the posterior wall of vestibulum	Smooth, semicircular lateral extension	Absent	Large, tongue-like, upper edge rounded	NA	NA
Mid-ventral band[a]	Extends from lower 1/2 to antapex	Extends from lower 1/2 to antapex	Absent	Present	NA	NA
Inner periplast component	Discrete hexagonal plates, anteriorly stepped	Slightly elongated hexagonal plates in longitudinal rows	Sheet without plates	Hexagonal plates covering entire cell surface	Sheet without plates	NA
Cytogenesis	Pole reversal	Pole reversal	NA	NA	NA	NA
Culture color	Pinkish-brown to yellow-greenish	Bright red to yellow and green	Deep red to yellow and green	Light brownish	*Yellow-orange to* reddish orange and olive yellow	Green-brownish to brown-pinkish
Phycobilin[c]	PE 545	PE 545	PE 545	NA	PE 545	NA

NA, no data available; [a]characters currently used to delineate genera in the family Geminigeraceae, [b]as seen from line-drawing; [c]spectrophotometry of live cells; [d]this study; [e]Hill and Wetherbee 1986; [f]Cerino and Zingone 2006; [g]Novarino 1991; [h]Butcher 1967 (as *Cryptomonas pseudobaltica*); [i]Rouchijajnen 1970.

described for both typical *P. sulcata* morphs (Cerino and Zingone 2006; Hill and Wetherbee 1986) and for *P. agilis*. The cells of *P. pseudobaltica* differ in size, shape, and structure of the inner periplast component (Table 3). Furthermore, *P. pseudobaltica* has never been studied by molecular techniques. Even on the basis of morphology alone, this taxon does not appear to belong to the genus *Proteomonas* (Deane et al. 2002). Among the morphological characters of *P. agilis* distinguished by LM and SEM (Table 3; Figures 1 and 2), few differ from those of *P. sulcata* haplomorph (Cerino and Zingone 2006; Hill and Wetherbee 1986). These species differ in cell size and proportions, with *P. sulcata* possessing larger hexagonal plates than *P. agilis*. The vestibular plate in *P. agilis* is much smaller, less prominent, and with a straight cut upper edge compared to the large, tongue-like plate with rounded upper edge observed in *P. sulcata* haplomorph (Cerino and Zingone 2006). It is uncertain whether *P. agilis* is conspecific with the previously described *Cryptomonas flexa* from the same locality (Rouchijajnen 1970), as the original description of *C. flexa* is too brief, morphological data on the internal structure of the periplast are lacking, and no molecular data are available.

The map of geographical distribution of various cultured *Proteomonas* strains of known origin in different culture collections is shown in Figure 6. To summarize, in most cases so far, we can either find various cultured strains in different culture collections, named *Proteomonas* spp. and isolated from coastal and open waters of Atlantic and Pacific oceans, Red Sea, etc., without any molecular data available; or, alternatively, different sequences of uncultured strains, also named *Proteomonas* spp. with unknown morphology, are present in GenBank. Several *P. sulcata* strains from the Stazione Zoologica di Napoli (SZN) culture collection, registered as typical of late autumn–winter cryptophytes in the Mediterranean coastal waters, have been described morphologically by LM and SEM (Cerino and Zingone 2006; see Table 3). However, molecular data for most of these strains have not been presented by the authors, and only SSU rDNA sequences of some SZN *Proteomonas* strains are available among the GenBank sequences. ITS2 sequences from any of the SZN *Proteomonas* strains were not available in GenBank at the time of analysis. Additionally, the SRA libraries for these strains were not found, making it impossible to assemble their ITS structure to compare with *P. agilis* sequences.

No signs of dimorphism were observed in *P. agilis* strain IBSS-4.14M, in contrast to *P. sulcata*. Cerino and Zingone (2006) did not observe a switch from one morph to another in separate cultures of both the haplomorph and the diplomorph strains of *P. sulcata*, as was noted previously for this species by Hill and Wetherbee (1986). Further investigations are necessary to determine if different culture conditions are required to induce a switch to another morphological stage in the same strain. It is also important to verify the ploidy of the cell populations in cultures.

Proteomonas was long considered monotypic since the original description of the genus by Hill and Wetherbee (1986). The type species, *P. sulcata*, was recognized as a unique cryptophyte due to both its variable morphology of alternating haplomorph and diplomorph life stages and phylogenetic position (Deane et al. 2002; Marin et al. 1998). Previous phylogenetic analyses based on complete nuclear-encoded SSU rRNA sequences (Marin et al. 1998) suggested that *P. sulcata* formed an independent lineage (referred to as clade V) with no significant affinity to any other clade. Its relationship to other clades appears to be unresolved by SSU rRNA. Recently performed three-genome phylogenetic

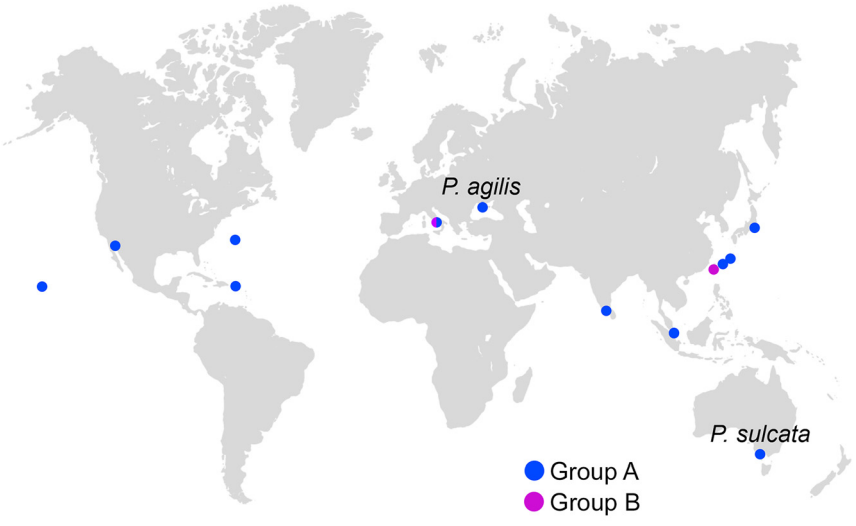

Figure 6: Geographical distribution of *Proteomonas* strains (group A and group B in Figure 3) worldwide.

analysis based on ultraconserved elements from the nuclear, nucleomorph, and plastid genomes (Greenwold et al. 2023) also found *Proteomonas* clade (referred to as clade 2B) as sufficiently distinct to justify its independence and to attributed its own subfamily, Proteomonadoideae. Our molecular phylogenetic analysis reliably placed novel taxon within the *Proteomonas* monophyletic genus based on 18S, 5.8S, and 28S gene sequences. However, these genes, previously considered the main phylogenetic markers for microalgae, have proven to be ineffective in distinguishing species within the cryptophyte clade, including monophyletic genera such as *Proteomonas*.

The present study utilized variable ITS spacers to improve the tree topology of *Proteomonas* strains and enhance the phylogenetic signal. The CBC approach and the search for compensatory substitutions in conservative ITS2 regions (Wolf et al. 2013) appeared to be a more reliable tool for differentiating cryptophyte species. Our results support the effectiveness of this approach in distinguishing closely related cryptophytes, including those of the *Proteomonas* genus.

Our data revealed undoubtedly that the genus *Proteomonas* is not monotypic but includes a range of unstudied species, in addition to the type species *P. sulcata* and *P. agilis* sp. nov. described in this study. The nucleotide sequences of nuclear ITS2 (Figure 5) and CBCs (Table 2) differentiate two Proteomonas strains, NIES-1375 and NIES-1005, from each other and distinguish them from other species of the genus found in various collections and the GenBank database. However, there are currently no morphological descriptions to support this idea. Meanwhile, the concept that ITS2 sequences of two distinct biological species differ by at least a single CBC (Coleman 2000; Müller et al. 2007; Wolf et al. 2013) suggests that strains NIES-1375 and NIES-1005 should be considered separate species of the genus *Proteomonas*. Numerous *Proteomonas* strains found worldwide require careful investigation by an international team using an integrated approach. The search for other cryptophytes that alternate different morphotypes, such as *P. sulcata*, is ongoing.

Acknowledgments: We are grateful to our colleagues, IBSS researchers T.V. Efimova, N.A. Moiseeva, and E.Y. Skorokhod for giving us a permission to present here part of our joint data on spectrophotometry of the cryptophyte strain IBSS-Cr-4.14M. We thank Dmitry V. Moiseenko for technical assistance in microalgae cultivation and Vyacheslav N. Lishaev (IBSS) for technical assistance with SEM. We would like to express our gratitude to the Editor in Chief, Prof. Matthew J. Dring, and the two anonymous reviewers for their valuable and constructive comments and suggestions, which have helped us to improve the quality of the manuscript.

Research ethics: All research procedures were conducted in accordance with local laws. All data were obtained and collected in accordance with local research protocols.

Informed consent: Not applicable.

Author contributions: A. N. Khanaychenko: original concept, methodology, culture establishment and maintenance, light microscopy, drafting and editing manuscript; O. V. Nikolaeva: DNA extraction and sequencing, molecular analyses, drafting and editing manuscript; O. A. Rylkova: electron microscopy; M. Saburova: visualization, review and editing manuscript; V. V. Aleoshin: methodology, analysis of molecular data, review and editing manuscript. All authors discussed the results and contributed to the final manuscript. The authors have accepted responsibility for the entire content of this manuscript and approved its submission.

Use of Large Language Models, AI and Machine Learning Tools: None declared.

Conflict of interest: The authors state no conflict of interest.

Research funding: This work was financially supported by the Research Program of the Russian Academy of Sciences grant agreement # 124022400152-1 and # 124021300070-2 at the IBSS RAS (AK, OR) and # AAAA-A17-117120540067-0 (ON, VA).

Data availability: Partial nuclear encoded 18S (SSU) and 28S (LSU) rDNA and complete internal transcribed spacer (ITS) regions were deposited in the GenBank with accession number OR687719.

References

Adolf, J.E., Yeager, C.L., Miller, W.D., Mallonee, M.E., and Harding, Jr., L.W. (2006). Environmental forcing of phytoplankton floral composition, biomass, and primary productivity in Chesapeake Bay, USA. *Estuar. Coast Shelf Sci.* 67: 108–122.

Aganesova, L.O. (2021). The reproduction and development of brackish-water copepods that were fed microalgae of different species. *Russ. J. Mar. Biol.* 47: 114–120.

Altenburger, A., Blossom, H.E., Garcia-Cuetos, L., Jakobsen, H.H., Carstensen, J., Lundholm, N., Hansen, P.J., Moestrup, Ø., and Haraguchi, L. (2020). Dimorphism in cryptophytes – the case of *Teleaulax amphioxeia/Plagioselmis prolonga* and its ecological implications. *Sci. Adv.* 6: 1–9.

Andersen, R.A. (2005). *Algae culturing technique*. Elsevier Academic Press, New York.

Bankevich, A., Nurk, S., Antipov, D., Gurevich, A.A., Dvorkin, M., Kulikov, A.S., Lesin, V.M., Nikolenko, S.I., Pham, S., Prjibelski, A.D., et al. (2012). SPAdes: a new genome assembly algorithm and its applications to single-cell sequencing. *J. Comput. Biol.* 19: 455–477.

Barkhatov, Y.V., Khromechek, E.B., Zykov, V.V., and Rogozin, D.Y. (2022). Cryptophytes of Lake Shira (Khakassia, Russia): explosive growth during breakdown of meromixis. *Hydrobiologia* 849: 3373–3387.

Bermúdez, J., Rosales, N., Loreto, C., Briceño, B., and Morales, E. (2004). Exopolysaccharide, pigment and protein production by the marine microalga *Chroomonas* sp. in semicontinuous cultures. *World J. Microbiol. Biotechnol.* 20: 179–183.

Bistricki, T. and Munawar, M. (1978). A rapid preparation method for scanning electron microscopy of Lugol preserved algae. *J. Microsc.* 114: 215–218.

Bolger, A.M., Lohse, M., and Usadel, B. (2014). Trimmomatic: a flexible trimmer for Illumina sequence data. *Bioinformatics* 30: 2114–2120.

Butcher, R.W. (1967). *An introductory account of the smaller algae of British coastal waters. Part IV: Cryptophyceae*. Fishery Investigations. Ministry of Agriculture, Fisheries & Food, Ser. IV, London, pp. 1–54.

Cerino, F. and Zingone, A. (2006). A survey of cryptomonad diversity and seasonality at a coastal Mediterranean site. *Eur. J. Phycol.* 41: 363–378.

Clay, B.L., Kugrens, P., and Lee, R.E. (1999). A revised classification of Cryptophyta. *Bot. J. Linn. Soc.* 131: 131–151.

Cloern, J.E. and Dufford, R. (2005). Phytoplankton community ecology: principles applied in San Francisco Bay. *Mar. Ecol. Prog. Ser.* 285: 11–28.

Coleman, A.W. (2000). The significance of a coincidence between evolutionary landmarks found in mating affinity and a DNA sequence. *Protist* 151: 1–9.

Coleman, A.W. (2007). Pan-eukaryote ITS2 homologies revealed by RNA secondary structure. *Nucleic Acids Res.* 35: 3322–3329.

Coutinho, P., Ferreira, M., Freire, I., and Otero, A. (2020). Enriching rotifers with "premium" microalgae: *Rhodomonas lens*. *Mar. Biotechnol.* 22: 118–129.

Daugbjerg, N., Norlin, A., and Lovejoy, C. (2018). *Baffinella frigidus* gen. et sp. nov. (Baffinellaceae fam. nov., Cryptophyceae) from Baffin Bay: Morphology, pigment profile, phylogeny, and growth rate response to three abiotic factors. *J. Phycol.* 54: 665–680.

Deane, J.A., Strachan, I.M., Saunders, G.W., Hill, D.R., and McFadden, G.I. (2002). Cryptomonad evolution: nuclear 18S rDNA phylogeny versus cell morphology and pigmentation. *J. Phycol.* 38: 1236–1244.

Dolgin, A. and Adolf, J. (2019). Scanning electron microscopy of phytoplankton: achieving high quality images through the use of safer alternative chemical fixatives. *J. Young Investig.* 37: 1–9.

Dunstan, G.A., Brown, M.R., and Volkman, J.K. (2005). Cryptophyceae and rhodophyceae; chemotaxonomy, phylogeny, and application. *Phytochemistry* 66: 2557–2570.

Efimova, T., Churilova, T., and Mukhanov, V. (2020). The influence of light of different spectral qualities on the photosynthetic characteristics of C-phycocyanine-containing cyanobacteria *Synechococcus* sp. WH5701. *Russ. J. Mar. Biol.* 46: 105–112.

Gervais, F. (1998). Ecology of cryptophytes coexisting near a freshwater chemocline. *Freshw. Biol.* 39: 61–78.

Greenwold, M.J., Cunningham, B.R., Lachenmyer, E.M., Pullman, J.M., Richardson, T.L., and Dudycha, J.L. (2019). Diversification of light capture ability was accompanied by the evolution of phycobiliproteins in cryptophyte algae. *Proc. Biol. Sci.* 286: 20190655.

Greenwold, M.J., Merritt, K., Richardson, T.L., and Dudycha, J.L. (2023). A three-genome ultraconserved element phylogeny of Cryptophytes. *Protist* 174: 125994.

Gusev, E., Podunay, Y., Martynenko, N., Shkurina, N., and Kulikovskiy, M. (2020). Taxonomic studies of *Cryptomonas lundii* clade (Cryptophyta: Cryptophyceae) with description of a new species from Vietnam. *Fottea* 20: 137–143.

Hammer, A., Schumann, R., and Schubert, H. (2002). Light and temperature acclimation of *Rhodomonas salina* (Cryptophyceae): photosynthetic performance. *Aquat. Microb. Ecol.* 29: 287–296.

Han, M.S. and Furuya, K. (2000). Size and species-specific primary productivity and community structure of phytoplankton in Tokyo Bay. *J. Plank. Res.* 22: 1221–1235.

He, X. and Peng, X. (2012). Spatial variability of summer and autumn phytoplankton community structure in Xiamen Western Bay based on pigment analysis. *Acta Oceanol. Sin.* 31: 165–175.

Hill, D.R.A. and Wetherbee, R. (1986). *Proteomonas sulcata* gen. et sp. nov. (Cryptophyceae), a cryptomonad with two morphologically distinct and alternating forms. *Phycologia* 25: 521–543.

Hoef-Emden, K. (2018). Revision of the genus *Chroomonas* Hansgirg: the benefits of DNA-containing specimens. *Protist* 169: 662–681.

Hoef-Emden, K. and Archibald, J.M. (2017) Cryptophyta (cryptomonads). In: Archibald, J.M., Simpson, A.G.B., and Slamovits, C.H. (Eds.). *Handbook of the protists*. Springer International Publishing, Cham, Switzerland, pp. 851–891.

Hoef-Emden, K. and Melkonian, M. (2003). Revision of the genus *Cryptomonas* (Cryptophyceae): a combination of molecular phylogeny and morphology provides insights into a long-hidden dimorphism. *Protist* 154: 371–409.

Hoef-Emden, K., Marin, B., and Melkonian, M. (2002). Nuclear and nucleomorph SSU rDNA phylogeny in the cryptophyta and the evolution of cryptophyte diversity. *J. Mol. Evol.* 55: 161–179.

Hu, H.-J., Li, Y.-G., Wu, L.-P., and Qi, Y.-Z. (2002). Studies on genus *Cryptomonas* from China Sea. *Acta Oceanol. Sin.* 21: 535–540.

Huang, B., Liu, Y., Xiang, W., Tian, H., Liu, H., Cao, Z., and Hong, H. (2008). Grazing impact of microzooplankton on phytoplankton in the Xiamen Bay using pigment-specific dilution technique. *Acta Oceanol. Sin.* 27: 147–162.

Johnson, M.D., Beaudoin, D.J., Laza-Martínez, A., Dyhrman, S.T., Fensin, E., Lin, S., Merculief, A., Nagai, S., Pompeu, M., Setälä, O., et al. (2016). The genetic diversity of *Mesodinium* and associated cryptophytes. *Front. Microbiol.* 7: 2017.

Khanaychenko, A., Mukhanov, V., Aganesova, L., Besiktepe, S., and Gavrilova, N. (2018). Grazing and feeding selectivity of *Oithona davisae* in the Black Sea: importance of cryptophytes. *Turk. J. Fish. Aquat. Sci.* 18: 937–949.

Khanaychenko, A.N., Rylkova, O.A., Aganesova, L.O., Popova, O.V., Aleoshin, V.V., and Saburova, M. (2022). *Rhodomonas storeatuloformis* sp. nov.(Cryptophyceae, Pyrenomonadaceae), a new cryptomonad from the Black Sea: morphology versus molecular phylogeny. *Fottea* 22: 122–136.

Kim, H.S., Kim, J.H., Jo, S.G., Rho, J.R., and Yih, W. (2020). Amino acids and fatty acids composition in mass-cultured *Teleaulax amphioxeia* strains with notable potential for rotifer (*Brachionus plicatilis*) enrichment. *J. World Aquacult. Soc.* 51: 712–728.

Kjer, K.M., Blahnik, R.J., and Holzenthal, R.W. (2001). Phylogeny of *Trichoptera* (Caddisflies): characterization of signal and noise within multiple datasets. *Syst. Biol.* 50: 781–816.

Klaveness, D. (1989). Biology and ecology of the Cryptophyceae: status and challenges. *Biol. Oceanogr.* 6: 257–270.

Krasnova, E.D., Pantyulin, A.N., Matorin, D.N., Todorenko, D.A., Belevich, T.A., Milyutina, I.A., and Voronov, D.A. (2014). Cryptomonad alga *Rhodomonas* sp. (Cryptophyta, Pyrenomonadaceae) bloom in the redox zone of the basins separating from the White Sea. *Microbiology* 83: 270–277.

Latsos, C., van Houcke, J., Blommaert, L., Verbeeke, G.P., Kromkamp, J., and Timmermans, K.R. (2021). Effect of light quality and quantity on productivity and phycoerythrin concentration in the cryptophyte *Rhodomonas* sp. *J. Appl. Phycol.* 33: 729–741.

Laza-Martínez, A. (2012). *Urgorri complanatus* gen. et sp. nov. (Cryptophyceae), a red-tide-forming species in brackish waters. *J. Phycol.* 48: 423–435.

Laza-Martínez, A., Arluzea, J., Miguel, I., and Orive, E. (2012). Morphological and molecular characterization of *Teleaulax gracilis* sp. nov. and *T. minuta* sp. nov. (Cryptophyceae). *Phycologia* 51: 649–661.

Łukaszek, M. and Hoef-Emden, K. (2017). The use of integrative taxonomy for identification of cryptophytes – first records for Poland. *Phycologia* 56: 122–123.

Magalhães, K., Santos, A.L., Vaulot, D., and Oliveira, M.C. (2021). *Hemiselmis aquamarina* sp.nov. (Cryptomonadales, Cryptophyceae), a cryptophyte with a novel phycobiliprotein type (Cr-PC 564). *Protist* 172: 125832.

Majaneva, M., Remonen, I., Rintala, J.M., Belevich, I., Kremp, A., Setälä, O., Jokitalo, E., and Blomster, J. (2014). *Rhinomonas nottbecki* n. sp. (Cryptomonadales) and molecular phylogeny of the family Pyrenomonadaceae. *J. Eukaryot. Microbiol.* 61: 480–492.

Marin, B., Klingberg, M., and Melkonian, M. (1998). Phylogenetic relationships among the Cryptophyta: analyses of nuclear-encoded SSU rRNA sequences support the monophyly of extant plastid-containing lineages. *Protist* 149: 265–276.

Martynenko, N., Kezlya, E., and Gusev, E. (2022). Description of a new species of the genus *Cryptomonas* (Cryptophyceae: Cryptomonadales), isolated from soils in a tropical forest. *Diversity* 14: 1001.

Medina, M., Collins, A.G., Silberman, J.D., and Sogin, M.L. (2001). Evaluating hypotheses of basal animal phylogeny using complete sequences of large and small subunit rRNA. *Proc. Natl. Acad. Sci. U. S. A.* 98: 9707–9712.

Medlin, L., Elwood, H.J., Stickel, S., and Sogin, M.L. (1988). The characterization of enzymatically amplified eukaryotic 16S-like rRNA-coding regions. *Gene* 71: 491–499.

Medlin, L.K., Piwosz, K., and Metfies, K. (2017). Uncovering hidden biodiversity in the Cryptophyta: clone library studies at the Helgoland time series site in the Southern German Bight indentifies the cryptophycean clade potentially responsible for the majority of its genetic diversity during the spring bloom. *Vie Milieu/Life Environ.* 67: 27–32.

Mikaelyan, A.S., Mosharov, S.A., Kubryakov, A.A., Pautova, L.A., Fedorov, A., and Chasovnikov, V.K. (2020). The impact of physical processes on taxonomic composition, distribution and growth of phytoplankton in the open Black Sea. *J. Mar. Syst.* 208: 103368.

Mikaelyan, A.S., Pautova, L.A., and Fedorov, A.V. (2021). Seasonal evolution of deep phytoplankton assemblages in the Black Sea. *J. Sea Res.* 178: 102125.

Mitchell, B.G. and Kiefer, D.A. (1988). Chlorophyll *a* specific absorption and fluorescence excitation spectra for light-limited phytoplankton. *Deep-Sea Res. A: Oceanogr. Res. Pap.* 35: 639–663.

Moncheva, S., Boicenco, L., Mikaelyan, A.S., Zotov, A., Dereziuk, N., Gvarishvili, C., Slabakova, N., Mavrodieva, R., Vlas, O., Pautova, L.A., et al. (2019) Phytoplankton. In: *Black Sea state of environment report 2009-2014/5*. Commission on the Protection of the Black Sea against Pollution, Istanbul, pp. 225–284.

Moorhouse, H., Read, D., Mcgowan, S., Wagner, M., Roberts, C., Armstrong, L., Nicholls, D., Wickham, H., Hutchins, M., and Bowes, M. (2018). Characterisation of a major phytoplankton bloom in the River Thames (UK) using flow cytometry and high performance liquid chromatography. *Sci. Total Environ.* 624: 366–376.

Müller, T., Philippi, N., Dandekar, T., Schultz, J., and Wolf, M. (2007). Distinguishing species. *RNA* 13: 1469–1472.

Nguyen, L.T., Schmidt, H.A., Von Haeseler, A., and Minh, B.Q. (2015). IQ-TREE: a fast and effective stochastic algorithm for estimating maximum-likelihood phylogenies. *Mol. Biol. Evol.* 32: 268–274.

Novarino, G. (1991). Observations on some new and interesting Cryptophyceae. *Nord. J. Bot.* 11: 599–611.

Oostlander, P.C., van Houcke, J., Wijffels, R.H., and Barbosa, M.J. (2020). Optimization of *Rhodomonas* sp. under continuous cultivation for industrial applications in aquaculture. *Algal Res*. 47: 101889.

Peltomaa, E., Johnson, M.D., and Taipale, S.J. (2018). Marine cryptophytes are great sources of EPA and DHA. *Mar. Drugs* 16: 1–11.

Polikarpov, I., Saburova, M., and Al-Yamani, F. (2020). Decadal changes in diversity and occurrence of microalgal blooms in the NW Arabian/Persian Gulf. *Deep Sea Res. II: Top. Stud. Oceanogr.* 179: 104810.

Rammel, T., Nagarkar, M., and Palenik, B. (2024). Temporal and spatial diversity and abundance of cryptophytes in San Diego coastal waters. *J. Phycol.* 60: 668–684.

Rouchijajnen, M.I. (1967). Species nova generis *Cryptomonas* (Pyrrophyta) e mari Nigro (Ponto Euxino). *Novitates Systematicae Plantarum non Vascularium (Novosti Sistematiki Nizshikh Rastenii)* 4: 71–73, (in Russian, with Latin diagnosis).

Rouchijajnen, M.I. (1970). Species novae generum *Cryptomonas* (Pyrrophyta) et *Platymonas* (Chlorophyta, Chlamydomonadales) e mari Nigro. *Novitates Systematicae Plantarum non Vascularium (Novosti Sistematiki Nizshikh Rastenii)* 7: 20–23, (in Russian, with Latin diagnosis).

Seixas, P., Coutinho, P., Ferreira, M., and Otero, A. (2009). Nutritional value of the cryptophyte *Rhodomonas lens* for *Artemia* sp. *J. Exp. Mar. Biol. Ecol.* 381: 1–9.

Shalchian-Tabrizi, K., Bråte, J., Logares, R., Klaveness, D., Berney, C., and Jakobsen, K.S. (2008). Diversification of unicellular eukaryotes: cryptomonad colonizations of marine and fresh waters inferred from revised 18S rRNA phylogeny. *Environ. Microbiol.* 10: 2635–2644.

Simdyanov, T.G., Diakin, A.Y., and Aleoshin, V.V. (2015). Ultrastructure and 28S rDNA phylogeny of two gregarines: *Cephaloidophora* cf. *communis* and *Heliospora* cf. *longissima* with remarks on gregarine morphology and phylogenetic analysis. *Acta Protozool.* 54: 241–262.

Simdyanov, T.G., Guillou, L., Diakin, A.Y., Mikhailov, K.V., Schrével, J., and Aleoshin, V.V. (2017). A new view on the morphology and phylogeny of eugregarines suggested by the evidence from the gregarine *Ancorasagittata* (Leuckart, 1860) Labbé, 1899 (Apicomplexa: Eugregarinida). *PeerJ* 5: e3354.

Solarska, M., Adamski, M., and Piątek, J. (2023). Complicated family relationships, or about taxonomic problems in the family Pyrenomonadaceae (Cryptophyceae). *Oceanol. Hydrobiol. Stud.* 52: 299–306.

Sun, Y., Youn, S.H., Kim, Y., Kang, J.J., Lee, D., Kim, K., Jang, H.K., Jo, N., Yun, M.S., Song, S.K., et al. (2022). Interannual variation in phytoplankton community driven by environmental factors in the northern East China Sea. *Front. Mar. Sci.* 9: 769497.

Šupraha, L., Bosak, S., Ljubešić, Z., Mihanović, H., Olujić, G., Mikac, I., and Viličić, D. (2014). Cryptophyte bloom in a Mediterranean estuary: high abundance of *Plagioselmis* cf. *prolonga* in the Krka river estuary (eastern Adriatic Sea). *Sci. Mar.* 78: 329–338.

Van der Auwera, G., Chapelle, S., and De Wachter, R. (1994). Structure of the large ribosomal subunit RNA of *Phytophtora megasperma*, and phylogeny of the oomycetes. *FEBS Lett.* 338: 133–136.

Vu, M.T., Douëtte, C., Rayner, T.A., Thoisen, C., Nielsen, S.L., and Hansen, B.W. (2016). Optimization of photosynthesis, growth, and biochemical composition of the microalga *Rhodomonas salina* – an established diet for live feed copepods in aquaculture. *J. Appl. Phycol.* 28: 1485–1500.

Wolf, M., Chen, S., Song, J., Ankenbrand, M., and Müller, T. (2013). Compensatory base changes in ITS2 secondary structures correlate with the biological species concept despite intragenomic variability in ITS2 sequences – a proof of concept. *PLoS One* 8: e66726.

Xing, X.-L., Lin, X.-Y., Chen, C.-P., Gao, Y.-H., Liang, J.-R., Huang, H.-Z., Li, B.-Q., Ho, K.-C., and Qi, Y.-Z. (2008). Observations of several cryptomonad flagellates from China Sea by scanning electron microscopy. *J. Systemat. Evol.* 46: 205–212.

Zhang, J., Wu, C., Pellegrini, D., Romano, G., Esposito, F., Ianora, A., and Buttino, I. (2013). Effects of different monoalgal diets on egg production, hatching success and apoptosis induction in a Mediterranean population of the calanoid copepod *Acartia tonsa* (Dana). *Aquaculture* 400: 65–72.

Zuker, M. (2003). Mfold web server for nucleic acid folding and hybridization prediction. *Nucleic Acids Res*. 31: 3406–3415.

Supplementary Material: This article contains supplementary material (https://doi.org/10.1515/bot-2024-0039).

Bionotes

Antonina N. Khanaychenko
A.O. Kovalevsky Institute of Biology of the Southern Seas, Russian Academy of Sciences, Leninskii Ave., 38/3, Moscow, 119991, Russian Federation
a.khanaychenko@gmail.com

Antonina N. Khanaychenko (PhD) is a leading researcher at the Institute of Biology of the Southern Seas. Her research has focused on the culture of various marine microalgae, rotifers, and copepods, as well as their interactions with fish larvae. Over the past 5 years, she has established a novel culture collection of cryptomonad strains isolated from the Black Sea. She is currently engaged in research on various aspects of their taxonomy and ecology.

Olga A. Rylkova
A.O. Kovalevsky Institute of Biology of the Southern Seas, Russian Academy of Sciences, Leninskii Ave., 38/3, Moscow, 119991, Russian Federation
olga.rylkova@gmail.com

Olga A. Rylkova (PhD) is a senior researcher at the Institute of Biology of the Southern Seas. She has extensive experience working with a variety of microalgae and microflora associated with algal cultures. Over the past 5 years, she has focused her research on the morphological and physiological parameters of microalgae and bacteria, employing techniques such as flow cytometry, confocal laser microscopy, and scanning electron microscopy.

Maria Saburova
Environment and Life Sciences Research Center, Kuwait Institute for Scientific Research, P.O. BOX 1638, Salmiya 22017, Kuwait
msaburova@gmail.com

Maria Saburova (PhD) is a marine biologist with over 30 years of experience in the taxonomy and ecology of planktonic and benthic microalgae from a wide geographic range. Since 2005, she has been engaged in research on marine microalgae of the Persian Gulf as a long-term scientific consultant at the Kuwait Institute for Scientific Research. Her research interests are focused on microalgal biodiversity, taxonomy, and ecology, with a particular emphasis on harmful bloom species and their impact on coastal ecosystems.